New Phytologist

Functional differences in transport properties of natural HKT1;1 variants influence shoot Na^+ exclusion in grapevine rootstocks.

Journal:	*New Phytologist*
Manuscript ID	NPH-MS-2017-25078.R1
Manuscript Type:	MS - Regular Manuscript
Date Submitted by the Author:	n/a
Complete List of Authors:	Henderson, Sam; University of Adelaide, School of Agriculture, Food and Wine Dunlevy, Jake; CSIRO, Agriculture and Food Wu, Yue; University of Adelaide, ARC Centre of Excellence in Plant Energy Biology Blackmore, Deidre; CSIRO, Agriculture and Food Walker, Rob; CSIRO, Agriculture and Food Edwards, Everard; CSIRO , Plant Industry Gilliham, Matthew; University of Adelaide, ARC Centre of Excellence in Plant Energy Biology Walker, Amanda; CSIRO, Agriculture and Food
Key Words:	hybrids, K51-40, North American rootstocks, 140 Ruggeri, site directed mutagensis, yeast, Xenopus laevis oocytes, salinity

Functional differences in transport properties of natural HKT1;1 variants influence shoot Na^+ exclusion in grapevine rootstocks

Sam W. Henderson[1,§], Jake D. Dunlevy[2,§], Yue Wu[1], Deidre H. Blackmore[2], Rob R. Walker[2], Everard J. Edwards[2], Matthew Gilliham[1,*] and Amanda R. Walker[2*]

[1] ARC Centre of Excellence in Plant Energy Biology, School of Agriculture, Food and Wine, University of Adelaide, PMB1, Glen Osmond, South Australia 5064, Australia
[2] CSIRO Agriculture & Food, Locked Bag 2, Glen Osmond, South Australia 5064, Australia

[§] These authors contributed equally
[*] Authors for correspondence:

Matthew Gilliham
Telephone: +61 8 8313 8145
Email: matthew.gilliham@adelaide.edu.au

Amanda R. Walker
Telephone: +61 8 83038629
Email: mandy.walker@csiro.au

Total word count: 6629

Word counts for each section:
- Introduction: 962
- Materials and Methods: 1731
- Results: 2226
- Discussion: 1538
- Acknowledgements: 165

Number of figures: 5

Colour Figures: 1, 2, 3, and 5

Number of tables: 0

Supporting information
- Tables: 4
- Figures: 12

Summary

- Under salinity, *Vitis spp.* rootstocks can mediate salt (NaCl) exclusion from grafted *Vitis vinifera* scions enabling higher grapevine yields and production of superior wines with lower salt content. Until now, the genetic and mechanistic elements controlling sodium (Na^+) exclusion in grapevine were unknown.
- Using a cross between two *Vitis* interspecific hybrid rootstocks we mapped a dominant quantitative trait loci (QTL) associated with leaf Na^+ exclusion (*NaE*) under salinity stress. The *NaE* locus encodes six high affinity potassium transporters (HKT). Transcript profiling and functional characterisation in heterologous systems identified *VisHKT1;1* as the best candidate gene for controlling leaf Na^+ exclusion.
- We characterised four proteins encoded by unique *VisHKT1;1* alleles from the parents, and revealed that the dominant HKT variants exhibit greater Na^+ conductance with less rectification than the recessive variants. Mutagenesis of VisHKT1;1, and TaHKT1.5-D from bread wheat, demonstrated that charged amino acid residues in the eighth predicted transmembrane domain of HKT proteins reduces inward Na^+ conductance, and causes inward rectification of Na^+ transport.
- The origin of the recessive *VisHKT1;1* alleles was traced to *V. champinii* and *V. rupestris*. We propose the genetic and functional data presented here will assist with breeding Na^+-tolerant grapevine rootstocks.

Keywords

hybrids, K51-40, North American rootstocks, 140 Ruggeri, site directed mutagenesis, salinity; yeast; *Xenopus laevis* oocytes.

Introduction

Saline soils and irrigation water reduce growth and productivity of crop species worldwide, which has negative economic, environmental, and social impacts (Pannell, 2001; Munns & Gilliham, 2015). Grapevine (*Vitis vinifera* L.) is moderately sensitive to irrigation water and soil salinity (Maas & Hoffman, 1977), suffering decreased growth and yield (Prior *et al.*, 1992; Walker *et al.*, 2002; Stevens *et al.*, 2011). In addition, fruit and wine quality can be reduced due to the accumulation of sodium (Na^+) and chloride (Cl^-) ions in berries (Li *et al.*, 2013). Unfavourable salty and soapy attributes in wine are associated with excessive wine Na^+ and Cl^- concentrations (Walker *et al.*, 2003; de Loryn *et al.*, 2014), while high salt concentrations in grape juice reduce fermentation efficiency by decreasing the viability of wine yeasts, and result in undesirable increases in acetic acid content of wine (Donkin *et al.*, 2010). Some countries impose legal limits for Na^+ and Cl^- concentrations permissible in wines (Leske *et al.*, 1997; de Loryn *et al.*, 2014). The Organisation Internationale de la Vigne et du Vin (OIV) recommends a maximum free Na^+ concentration of 60 mg/L in wine (Stockley & Lloyd-Davies, 2001). Wineries often reject fruit with Na^+ levels above this level. Growers may attempt to negate salinity in vineyards by flushing salts from soils with large volumes of irrigation water. However, this practice is not economically viable or practical in regions with limited quality water – a problem expected to worsen with climate change (Elliott *et al.*, 2014). A more cost effective and efficient approach to limit the effects of salinity on grapevines is by grafting onto rootstocks that can restrict root-to-shoot transport of Na^+ and Cl^-, a trait referred to as shoot ion exclusion. As wineries use Na^+ concentrations in berries and grape juice as a basis for rejection, finding a genetic solution for shoot Na^+ accumulation in grapevine would be advantageous to the wine industry so it can maintain quality wine production in salt-affected regions.

Grapevine rootstocks derived from wild North American *Vitis* species were first used in viticulture in the late 19th Century to provide resistance to the soil-born parasite phylloxera, which destroyed vineyards throughout Europe, an episode called the Great French Wine Blight (Stevenson, 1980). An estimated 80% of vines in vineyards worldwide are now grafted onto interspecific rootstocks (Ollat *et al.*, 2016).

Rootstocks are selected for beneficial traits including phylloxera resistance (Benheim *et al.*, 2012), nematode resistance (Ferris *et al.*, 2012), controlled vigour and yield (Walker *et al.*, 2002), drought resistance (Serra *et al.*, 2014) and ion exclusion (Tregeagle *et al.*, 2010). Rootstock breeding programs can utilize marker assisted selection to hasten the pyramiding of key rootstock traits into new elite genotypes (Ollat *et al.*, 2016), yet little is currently known about the genetic mechanisms controlling ion exclusion in grapevines.

Most grapevine studies have concentrated on Cl^- toxicity (Ehlig, 1960; Downton, 1977a; Walker *et al.*, 2004) and the mechanistic basis of Cl^- exclusion from shoots (Gong *et al.*, 2011; Henderson *et al.*, 2014; Fort *et al.*, 2015; Henderson *et al.*, 2015). In other crops, shoot Na^+ exclusion is more widely studied and it is acknowledged that the major component of both Na^+ and Cl^- exclusion from plant shoots occurs via root based mechanisms (Munns & Gilliham, 2015; Li *et al.*, 2017). As a result Na^+ exclusion from leaves correlates well with exclusion from berries (Figure S1; Walker *et al*., (2004)), and can be used as a proxy measure of whole shoot Na^+ exclusion *per se.*

QTLs for shoot Na^+ exclusion in bread wheat (*Kna1*), durum wheat (*Nax1* and *Nax2*), rice (*SKC1*) and tomato are underpinned by genes encoding high affinity potassium (K^+) transporter (HKT) proteins (Ren *et al.*, 2005; Byrt *et al.*, 2007; James *et al.*, 2011; Asins *et al.*, 2013). HKT proteins belong to the Ktr/TrK/HKT family of monovalent cation transporters present in plants, bacteria and fungi, but not in animals (Corratgé-Faillie *et al.*, 2010). Proteins from the HKT1 subgroup selectively transport Na^+ over other cations (Mäser *et al.*, 2002; Horie *et al.*, 2009; Waters *et al.*, 2013), and confer Na^+ exclusion from shoots through retrieval of Na^+ from root xylem vessels into surrounding xylem parenchyma cells (Sunarpi *et al.*, 2005; Davenport *et al.*, 2007; Møller *et al.*, 2009; Byrt *et al.*, 2014). Emerging evidence indicates that molecular mechanisms of HKT1-mediated salinity tolerance between plants may depend upon not only expression differences but in some cases subtle differences in functional properties, which may be attributed to single amino acid substitutions and possible allelic variations (Ren *et al.*, 2005; Rus *et al.*, 2006; Baxter *et al.*, 2010; Cotsaftis *et al.*, 2012; Ali *et al.*, 2016; Tounsi *et al.*, 2016). The benefits of identifying

natural variants of HKT has been demonstrated with HKT1.5 from salt-tolerant wheat *Triticum monococcum* which, when introgressed into salt-sensitive *Triticum durum*, increased grain yield on saline soil by 25% in the field (Munns *et al.*, 2012).

Here, we examine the genetic basis of Na^+ exclusion in grapevine. We take advantage of a family of heterozygous hybrid vines derived from a cross between two interspecific rootstock hybrids K51-40 (*V. champinii* x *V. riparia*) and 140 Ruggeri (*V. berlandieri* syn. *V. cinerea* var. Helleri x *V. rupestris*) that was previously shown to exhibit variation in leaf Na^+ by 30-fold (Gong *et al.*, 2014). We identified a QTL, named *NaE* for Na^+ exclusion, containing six closely located *HKT1* genes, of which one was expressed in roots and encoded a functional Na^+ transporter. Differences in *HKT1;1* alleles from the parent rootstocks were identified and used to investigate the importance of key amino acid residues contributing to differences in Na^+ transport properties and variation in shoot Na^+ exclusion in the hybrid progeny. The identified SNPs are being utilized by breeding programs for generating Na^+-excluding rootstock germplasm via marker assisted selection.

Materials and Methods

Grapevine material and Na^+ screens

A family of 40 hybrid rootstocks from a cross between K51-40 (*V. champinii* x *V. riparia*) and 140 Ruggeri (*V. berlandieri* x *V. rupestris*) (Gong *et al.*, 2011), together with both parents, were screened for leaf Na^+ exclusion ability in The Plant Accelerator Phenomics Facility, Adelaide, Australia in December 2013. Dormant cuttings were callused for two weeks at 28 °C (Yalumba Nursery, Nuriootpa, Australia) and transferred to a 50:50 sand:perlite mix under regular misting for four weeks to initiate root development. Rooted cuttings were transplanted into 1.8 kg of potting mix (6 mm Premium Mix Van Schaik's, BIOGRO, Mt Gambier, Australia) in 2.5 L pots, established for four weeks, then loaded onto The Plant Accelerator's conveyor belt. Prior to loading, vines were trimmed to a single shoot and axillary growth was continually removed. Each genotype consisted of three replicate vines, in three randomised blocks. Salt applications, consisting of 10:6:1:1 ratio of Cl^- :Na^+:Mg^{2+}:Ca^{2+}, were applied to pots in containers (to avoid run through) on days 1, 3 and 7, equating to soil Na^+ concentrations ramping from 21 to 42 to a final concentration of 60 mM. On all other days, the pots were automatically weighed and watered to a target weight to replace water lost through evapotranspiration, ensuring all pots maintained equivalent salt concentrations at full water capacity. On day 13, laminae of fully matured leaves of each vine were harvested and dried at 65 °C for 2 days. For determining Na^+ content, powdered sample (100 mg) was digested in 2 ml concentrated HNO_3 at 95 °C, diluted to 12 mL with deionised water, and analysed by CSIRO Analytical Services Unit (Adelaide) using inductively coupled plasma optical emission spectrophotometry (ThermoFisher, Cambridge, UK).

In a subsequent experiment in 2014, five selected hybrid progeny, the parents, accessions of the grandparent species, *V. champinii* 'Dogridge', *V. riparia* 'Gloire', *V. berlandieri* 'R1xMazade' and *V. rupestris* 'du Lot', and 10 common *V. vinifera* cultivars, were screened to compare Na^+ exclusion abilities. Establishment of cutting material and experimental conditions were similar to the first hybrid Na^+ screen, except final salt application occurred on day 8, and leaves were harvested on day 19.

174

175 **Linkage mapping and QTL analysis**

176 Genome wide single nucleotide polymorphism (SNP) data was generated by Diversity
177 Arrays Technology Pty Ltd (Canberra, Australia) using DArTSeq™ genotype by
178 sequencing (GBS). This uses PstI/TaqI restriction digestion of genomic DNA followed
179 by PstI-specific adapter targeted short-read sequencing using HiSeq2500 (Illumina,
180 USA). The DArTSeq methods were performed as described in Courtois *et al*., (2013),
181 except sequence reads were aligned to the grapevine reference genome (Jaillon *et*
182 *al.*, 2007). SNP markers aligned to the genome and those with call rates of 1 were
183 used to construct a consensus linkage map, in JoinMap® Version 4.1 software using
184 maximum likelihood mapping (Van Ooijen, 2006). A consensus framework of linkage
185 groups was obtained using a logarithm of odds (LOD) likelihood score between 3.0-
186 5.0, and the Haldane mapping function to calculate the genetic distance between
187 markers. Chromosome assignment of linkage groups was determined from the
188 alignment of DArTSeq SNP reads to the grapevine reference genome (Jaillon *et al.*,
189 2007). QTLs for sodium exclusion were investigated using interval mapping analysis
190 performed in MapQTL® Version 6 (Van Ooijen & Kyazma, 2009). The permutation
191 test was used to estimate the genome wide empirical threshold for QTL detection
192 based on LOD values of $P<0.01$. Interval mapping resulted in a single significant QTL.
193 To identify potential small modifying QTLs, multiple QTL mapping (MQM) analysis
194 was undertaken with the strongest marker from this QTL used as a cofactor. No
195 other significant QTLs were detected.

196

197 **Sequencing and cloning**

198 *VviHKT1;1* and *VviHKT1;3* coding sequences were PCR amplified from *V. vinifera* (cv
199 Cabernet Sauvignon) root cDNA using Phusion Polymerase (ThermoFisher Scientific)
200 and primers designed to these gene sequences (Table S1). Purified fragments were
201 ligated to pCR8/GW/TOPO. To identify polymorphisms in each genotype, the
202 *VisHKT1;1* gene was PCR amplified from K51-40 and 140 Ruggeri genomic DNA, and
203 sequenced (accession numbers in Table S2). Using polymorphisms as a reference,

coding sequences of *VisHKT1;1* allelic variants were PCR amplified from root cDNA of parent rootstocks using PfuUltra II Fusion HS DNA Polymerase (Agilent), and ligated to pENTR/D-TOPO. *VisHKT1;1-E*^{K} and *VisHKT1;1*-e^{K} were isolated from K51-40, and *VisHKT1;1-E*^{R} and *VisHKT1;1-e*^{R} from 140 Ruggeri. Cleavage amplified polymorphic sequence (CAPS) markers designed to score the inheritance of each allele are given in Table S3.

VviHKT1;1 sequences from *V. champinii*, *V. riparia*, *V. berlandieri*, *V. rupestris* and *V. vinifera* cultivars, Grenache, Merlot, Pinot noir, Shiraz, Chardonnay, Pinot gris, Riesling, Sauvignon blanc and Semillon were obtained by sequencing PCR products amplified from genomic DNA.

Subcellular localisation

V. vinifera (cv. Cabernet Sauvignon) *VviHKT1;1* without a stop codon was recombined with pMDC83 (Curtis & Grossniklaus, 2003) using LR Clonase II (Life Technologies) to generate 2x35S:*VviHKT1;1-GFP*. Plasmid ER-rk containing HDEL-mCherry (Nelson *et al.*, 2007) was used for co-localisation. Plasmid pUBN-GFP-DEST (Grefen *et al.*, 2010) was used to express cytosolic GFP. Plasmid pEAQ-HT-DEST harbouring p19 gene silencing suppressor was used to maximise expression (Sainsbury *et al.*, 2009). Vectors were incorporated into *Agrobacterium tumefaciens* (Agl-1) via freeze thawing. Overnight cultures of *A. tumefaciens* harbouring pMDC83-VviHKT1;1, ER-rk, pUBN-GFP-DEST or pEAQ-HT-DEST were resuspended in 10 mM $MgCl_2$, 150 µM acetosyringone and 10 mM MES pH 5.6. Cultures were combined as follows with final OD_{600} shown in brackets: pMDC83-VviHKT1;1 (0.5) and pEAQ-HT-DEST (0.2); pMDC83-VviHKT1;1 (0.5), ER-rk (0.2) and pEAQ-HT-DEST (0.2); pUBN-GFP-DEST (0.5) and pEAQ-HT-DEST (0.2). Bacterial suspensions were infiltrated into the abaxial side of fully expanded leaves of 5-week-old *Nicotiana benthamiana* with a 1 ml syringe. Leaf sections were imaged after two days using a Nikon A1R confocal laser scanning microscope with 63x water objective lens and NIS-Elements C software (Nikon Corporation, Tokyo, Japan). FM4-64 (Sigma) was used to infiltrate tobacco leaves and imaged after 10 minutes at room temperature. Under these

conditions, the plasma membrane (not endomembrane) is predominantly stained. Excitation/emission conditions were GFP (488 nm/ 500 – 550 nm), FM4-64 and mCherry (561 nm/ 570 – 620 nm).

Site directed mutagenesis

Site directed mutants of *VisHKT1;1* allelic variants were generated in yeast and *X. laevis* expression vectors. Mutagenesis was performed by inverse PCR of expression vectors using primers (see Table S1) with 15 bp overlaps at their 5' ends, and mutations incorporated within. Reactions contained 0.2 ng plasmid, 500 nM forward and reverse primers and 0.25 units Phusion Polymerase (ThermoFisher Scientific) in 25 µL. Reactions were treated with Cloning Enhancer (Clontech Laboratories Inc), and re-circularised using In-Fusion HD (Clontech Laboratories Inc).

Oocyte expression assays

cDNAs encoding *VisHKT1;1* variants were recombined into the *Xenopus laevis* expression vector pGEMHE-DEST, using LR Clonase II (Life Technologies). Plasmids were linearised with NheI or SbfI (New England Biolabs). Capped RNA (cRNA) was synthesised *in vitro* with mMessage mMachine T7 kit (Ambion) using linear plasmids as templates. cRNA was purified by phenol/chloroform extraction followed by ethanol precipitation and elution in water. Stage V and VI oocytes were injected with 42 nL cRNA (21 ng), or sterile water. Injected oocytes were incubated in calcium Ringers solution (96 mM NaCl, 2 mM KCl, 5 mM MgCl, 0.6 mM $CaCl_2$, 5 mM Hepes, 5% (v/v) horse serum, 500 µg.mL^{-1} tetracycline and 1 x penicillin-streptomycin (Sigma P4333)). Electrophysiology was performed 1 day after injection.

Electrophysiology

Whole-cell currents were recorded using two-electrode voltage clamping (TEVC) on a Roboocyte with integrated ClampAmp amplifier (Multichannel Systems). Electrodes were filled with 3 M KCl. Oocytes were perfused with solutions containing 1.8 mM $CaCl_2$, 6 mM $MgCl_2$, 10 mM MES, variable Na^+-gluconate, pH 5.5 (adjusted with Tris) and osmolality of 230 mOsm.kg^{-1} (adjusted with D-mannitol). From a holding

potential of -40 mV, oocytes were clamped stepwise from +60 mV to -140 mV in 20 mV decrements for 550 ms. Currents mediated by grapevine or wheat HKT1;1 were determined by subtracting mean currents of water injected controls from the same batch of oocytes in the same solutions.

Yeast assays

VisHKT1;1 variants, and VviHKT1;3 (Cabernet Sauvignon) were recombined into pYES-DEST52 using LR Clonase II (Life Technologies). *Saccharomyces cerevisiae* strain INVSc2 (MATa, *his3Δ-1*, *ura3-52*) was transformed with plasmids using the lithium acetate procedure. Transformants were selected on yeast nitrogen base (YNB) (Difco) without uracil, with 2% (w/v) D-glucose. For Na^+ toxicity assays, yeast was grown overnight in YNB without phosphates or NaCl (MP Biomedicals), supplemented with 1 $g.L^{-1}$ KH_2PO_4, 95 $mg.L^{-1}$ L-histidine-HCl, and 2% (w/v) D-glucose. Yeast was diluted to an OD_{600} of 1.0 in sterile water. 10-fold serial dilutions were prepared in sterile water, and 5 µL spotted onto plates containing YNB without phosphates and without NaCl (MP Biomedicals), supplemented with 1 $g.L^{-1}$ KH_2PO_4, 95 $mg.L^{-1}$ L -histidine-HCl, 1.5% (w/v) D-raffinose, 0.001 – 0.005% (w/v) D-galactose for induction and 0.25% phytagel (Sigma). The basal Na^+ concentration was approximately 500 µM from phytagel. For Na^+ toxicity screening, growth was monitored on media containing 50 mM NaCl. Control plates to demonstrate equal dilutions contained 2% (w/v) D-glucose. Plates were incubated at 28 °C for 3 days.

Quantitative real time PCR (qPCR)

RNA from root stele and root epidermis/cortex enriched tissue was prepared from grapevine rooted leaves as described previously (Henderson *et al.*, 2014). cDNA was synthesised from 0.5 µg total RNA using Superscript III (Life Technologies) following manufacturers procedures. qPCR was performed on a QuantStudio 12K Flex Real-Time PCR machine (Thermo Fisher Scientific). 10 µL qPCR reactions contained 250 nM forward and reverse primer, 1x KAPA SYBR FAST qPCR Master Mix (KAPA Biosystems), and 1 µL cDNA (diluted 1:4). Triplicate reactions were performed using 40 cycles of the following: 95 °C 1 sec, 55 °C 15 sec, 72 °C 5 sec. Melt curve analysis was performed to ensure a single band was amplified. Relative expression levels

were calculated using primer pair efficiencies (*E*) and normalised to *VvElongation-factor-1-α* using the formula ($E_{HKT1;1}^{\Delta ct}/E_{EF1\text{-}\alpha}^{\Delta ct}$).

VisHKT1;1 allele-specific qPCR reactions were performed using forward and reverse primers (Table S1) containing allele-specific SNPs in their 3` terminal base. Specificity was achieved by performing reactions as described above, except annealing at 63 °C. Allele copy number were estimated by interpolation from standard curves made from serial dilutions of linearised pGEM-HE plasmids quantified by UV-spectrophotometry. Data were normalised to cDNA volume. The sum of two allele copy numbers was compared to total copies of *VisHKT1;1* transcript using non-specific primers in the same samples.

Statistical analysis

Data were analysing GraphPad Prism version 7.00 for Windows (GraphPad). All data are presented as mean ±SEM. Means were compared using the different statistical tests described in the figure legends.

Results

Mapping a major QTL for Na^+ exclusion in a hybrid grapevine population

We aimed to detect QTL for leaf Na^+ exclusion in a population of hybrid rootstocks derived from a cross between K51-40 and 140 Ruggeri (Gong *et al.*, 2014). Forty hybrids were exposed to a mixed cation treatment for 13 days, and the lower leaves (lamina only) were harvested for analysis of Na^+ accumulation. A >40-fold difference in Na^+ accumulation was seen within the hybrid progeny with the lowest, 0.005% dry weight, and the highest, 0.213% dry weight, while two parents K51-40 and 140 Ruggeri had similar leaf Na^+ concentrations of 0.016 and 0.015% dry weight, respectively (Figure 1A). The transgressive variation seen in this near-Mendelian trait indicated it was probably heterozygous in each parent. A broad sense heritability score of 0.91 was estimated for Na^+ exclusion in this population suggesting a high degree of genetic control.

GBS was performed on the 40 hybrids and parents. Resulting SNP data was used to construct a consensus linkage map consisting of 514 SNP markers distributed over 19 linkage groups, at a mean interval of 5.3 cM (Figure S2). A single major QTL explaining up to 72% of the genetic variation in Na^+ exclusion was identified on chromosome 11, spanning a 42 cM region of approximately 14 Mb (Figure 1B). We named this locus *NaE*, for Na^+ exclusion. SNP markers underlying the peak of the *NaE* QTL were used to group the 40 hybrids based on their inheritance of this locus, and confirmed that the associated alleles were likely to be heterozygous in both parents (Figure 1A). This analysis revealed that the Na^+ exclusion trait is dominant over Na^+ accumulation, as hybrids with low Na^+ accumulation were generally associated with the inheritance of one or more dominant loci, designated as NaE^K and NaE^R for excluder locus derived from K51-40 and 140 Ruggeri. In contrast, high Na^+ accumulation was generally associated with the inheritance of two recessive loci, designated Nae^K and Nae^R (Figure 1A).

Based on the grapevine reference genome (Jaillon *et al.*, 2007), the *NaE* locus contains 583 genes (Table S4). Six *HKT1* genes were clustered within a 320 Kb region located close to the peak LOD score of the *NaE* locus (Figure 1B & C) and knowledge of Na^+ exclusion from other plant species suggested that members of the *HKT1* family were strong candidate genes.

Phylogenetic analysis of these grapevine HKT1s against HKTs from other plant species has been reported previously (Ali *et al.*, 2012). This showed that, of the well characterised HKTs, all grapevine HKT1s are most similar to rice OsHKT1;1. The grapevine HKT1s fall into two sub-clades, whereby VviHKT1;1, VviHKT1;2 and VviHKT1;3 share a degree of homology (53 to 63% identity) and VviHKT1;6. VviHKT1;7 and VviHKT1;8 share higher sequence similarity (85 to 97% identity) (Figure S3).

HKT1;1 is expressed in the root stele and encodes a Na^+ selective plasma membrane transporter

In wheat and Arabidopsis, HKT proteins in roots regulate Na^+ accumulation in shoots by controlling Na^+ retrieval from root xylem vessels (Davenport *et al.*, 2007; Munns *et al.*, 2012; Byrt *et al.*, 2014). We therefore mined genome-wide expression data to determine which grapevine *HKT1* transcripts were expressed in roots. Only two *HKT1* transcripts, *VviHKT1;1* and *VviHKT1;3* were highly abundant in whole roots of *V. vinifera*, and both transcripts were present at similar levels (Figure 2A). To identify whether *VviHKT1;1* and *VviHKT1;3* encoded Na^+ transport proteins, full length cDNAs corresponding to each protein were isolated and expressed in *X. laevis* oocytes. When oocytes were clamped at negative membrane potentials, VviHKT1;1 mediated large inward currents (2 µA at -140 mV) in the presence of 30 mM Na^+ (Figure 2B) whereas VviHKT1;3 did not increase currents above the level of the water control (Figure 2B). Furthermore, functional characterisation in yeast indicated *VviHKT1.3* did not function as a Na^+ transporter as its expression did not lead to inhibition of yeast growth on plates containing 50 mM Na^+ unlike *AtHKT1* (Figure S4). These findings implicate *HKT1;1* as a gene important for Na^+ exclusion in grapevine, while the function of *HKT1;3* remains unknown.

Quantitative PCR of root epidermal/cortical and stelar fractions of K51-40 and 140 Ruggeri showed *HKT1;1* transcripts were more abundant in the root stele of both genotypes (Figure 2C). Expression of *VviHKT1;1* with a C-terminal GFP tag in tobacco epidermis showed a strong signal that co-localised with the lipohilic dye FM4-64 at the plasma membrane, but did not co-localise with free cytoplasmic GFP, or the endoplasmic reticulum (ER) marker HDEL-mCherry (Figure 2D & E). These findings confirm that VviHKT1;1 protein is likely to be localised on the plasma membrane of grapevine root stelar cells.

Four unique *HKT1;1* alleles from K51-40 and 140 Ruggeri display different functional properties

HKT1;1 coding sequences were isolated from the two parents of the mapping population, K51-40 and 140 Ruggeri, and given the prefix *Vis* for *Vitis interspecific*. Four unique *VisHKT1.1* alleles were identified, two from each parent (Figure 3A & S5). CAPS markers designed to the *VisHKT1;1* alleles were used to score hybrids for their allelic inheritance. Resulting marker scores were identical to that of SNPs mapped nearby (Figure 1A); hence we named the *VisHKT1.1* alleles as per the associated *NaE* locus (*VisHKT1;1-E*^{K} and *VisHKT1;1-e*^{K} from K51-40; *VisHKT1;1-E*^{R} and *VisHKT1;1-e*^{R} from 140 Ruggeri). Eighteen amino acid differences were observed between encoded proteins of the four alleles (Figure 3A and Figure S5). Six polymorphic residues, at positions 106, 129, 163, 391, 534 and 537, were conserved between the two *VisHKT1;1-E* allelic variants and also between the two *VisHKT1;1-e* variants (Figure 3A).

To assess whether allele-specific expression contributes to the variation in Na^+ exclusion in the hybrid population, absolute transcript abundance of these four alleles in root fractions was quantified in the parents using allele-specific primers. Expression of *HKT1;1* alleles in root epidermal/cortical and stelar fractions, assayed by qPCR, showed *VisHKT1;1-E* alleles to be approximately 2-fold more abundant than *VisHKT1;1-e* alleles (Figure 3B). There were no differences in expression of *VisHKT1;1-E*^{K} and *VisHKT1;1-E*^{R} or between *VisHKT1;1-e*^{K} and *VisHKT1;1-e*^{R} alleles (Figure 3A). The sum of *VisHKT1;1-E* and *VisHKT1;1-e* transcript copy number was equivalent to total *VisHKT1;1* copy number using non-allele-specific *HKT1;1* primers in each sample, demonstrating that the PCR primers were highly allele-specific (Figure 3B).

For functional analysis, the *VisHKT1;1* alleles were first expressed in yeast. On control plates containing glucose, which represses gene expression, all strains grew at the same rate demonstrating equal dilution (Figure 3C). When *VisHKT1;1* allelic variants were expressed by substituting glucose with raffinose and galactose (which induces gene expression), all strains grew at a similar rate on low (0.5 mM) Na^+ (Figure 3C). Conversely, growth of yeast expressing *VisHKT1;1* allelic variants on induction medium was strongly inhibited by 50 mM

Na^+, while growth of yeast containing an empty vector was not inhibited (Figure 3C). This suggests that each grapevine VisHKT1;1 allelic variant transports Na^+ in yeast. Na^+-induced growth-inhibition was greater in yeast strains expressing *VisHKT1;1-E* variants compared to *VisHKT1;1-e* variants from both parents (Figure 3C), implying that VisHKT1;1-E proteins have higher Na^+ transport activity than VisHKT1;1-e proteins.

To confirm these differences, we performed TEVC of *X. laevis* oocytes injected with different VisHKT1;1 allelic variants. When perfused with 30 mM external Na^+ ($[Na^+]_{ext}$), VisHKT1;1-E variants mediated Na^+ transport in both directions across the oocyte membrane (Figure 3D). Conversely, both VisHKT1;1-e variants displayed inward rectification – characterised by inward currents at negative voltages but restricted outward currents at positive voltages (Figure 3D). We quantified inward rectification as the ratio between inward (-140 mV) and outward (+60 mV) chord conductance (G_{Na+}), where a ratio of 1 indicates equal G_{Na+} in both directions. From both rootstocks, VisHKT1;1-E variants had lower (approximately 50%) inward rectification ratios than VisHKT1;1-e, irrespective of $[Na^+]_{ext}$ (Figure S6). Inward rectification is an intrinsic property of grapevine VisHKT1;1-e variants, and not due to differences in $[Na^+]_{int}$, as increasing $[Na^+]_{ext}$ did not significantly alter the reversal potential (E_{rev}) between allelic variants, and E_{rev} followed a positive Nernstian shift (Figure S7). In addition to differences in inward rectification, we also observed differences in the inward current at physiologically relevant negative membrane potentials in plants (-140 to -80 mV) between the VisHKT1;1 variants (Figure 3D). To examine this in detail, we thouroghly investigated the difference between VisHKT1;1-E^K and VisHKT1;1-e^K, finding that the VisHKT1;1-E^K variant displayed ~25 % larger currents at -140 mV in 30 mM Na^+ solutions, and that this difference was consistent across different batches of oocytes (Figure S8).

We examined monovalent cation selectivity of different VisHKT1;1 allelic variants in oocytes. All variants were highly selective for Na^+, mediating large inward currents in 10 mM NaCl, each with an E_{rev} close to the predicted Nernst potential for this cation (Figure S9). When Na^+ was substituted for lithium (Li^+), potassium (K^+), rubidium (Rb^+) or cesium (Cs^+), all VisHKT1;1 allelic variants were unable to mediate inward currents (Figure S9). This demonstrates that all VisHKT1;1 allelic variants characterised here were selective only for Na^+.

Two polymorphisms (Ser-534-Arg and Gly-537-Asp) are responsible for differences in Na^+ conductance and rectification

Of six polymorphic residues conserved between VisHKT1;1-E and VisHKT1;1-e allelic variants, two residues occur in the predicted $M2_D$ transmembrane region near the carboxy (C)-terminus, where charged residues are important for correct functioning of plant and bacterial Trk/Ktr/HKT proteins (Kato *et al.*, 2007). In VisHKT1;1-E variants, these residues are uncharged, Ser-534 and Gly-537, but differ in VisHKT1;1-e variants with oppositely charged Arg-534 (positive) and Asp-537 (negative) (Figure 3A and S5). To investigate whether these SNPs affected protein function, we performed mutagenesis of VisHKT1;1-e^K to generate two single mutant proteins, VisHKT1;1-e^K_{D537G}, VisHKT1;1-e^K_{R534S}, and a double mutant protein VisHKT1;1-$e^K_{R534S/D537G}$. Expression of mutant alleles in oocytes revealed that the D537G mutation alone had no effect on G_{Na+} or rectification, as this protein behaved like original VisHKT1;1-e^K (Figure 4A; Figure S10). Conversely, single R534S mutation resulted in larger outward currents, reducing the inward rectification observed in VisHKT1;1-e^K, and also resulted in significantly higher inward slope G_{Na+} in oocytes compared to wild-type (Figure 4A, Figure S10). When R534S mutation was combined with D537G mutation in $e^K_{R534S/D537G}$, to mimic residues present at the C-terminus of VisHKT1;1-E variants, rectification was abolished and inward slope G_{Na+} was further increased compared to the e^K_{R534S} single mutant (Figure 4A) , but this increase was not statistically significant compared to the R534S single mutant (Figure S10). These mutations had no effect on cation selectivity of the e^K protein (Figure S11). Comparing the chord conductance ratio of each protein confirmed that Arg-534 is the rectification residue in VisHKT1;1, as e^K-wild-type and e^K_{D537G} variants had significantly higher ratios compared to e^K_{R534S} mutant and $e^K_{R534S/D537G}$ (Figure 4B). When expressed in yeast, both single mutant proteins inhibited growth on 50 mM Na^+ to the same degree as e^K-wild-type (Figure 4C). Only $e^K_{R534S/D537G}$ inhibited yeast growth on 50 mM Na^+ to the same degree as E^K-wild-type (Figure 4C). This suggests that variable yeast growth inhibition mediated by the VisHKT1;1 allelic variants is due to the larger inward Na^+ conductance of allele E variants and not due to differences in inward rectification. To further confirm the role of Arg-534 in rectification and reduced conductance of VisHKT1.1-e variants, we mutated the equivalent residue in wheat TaHKT1.5-D from serine to arginine.

This mutation greatly reduced the inward Na^+ conductance, with TaHKT1.5-D_{S506R} showing currents half the magnitude of wild-type TaHKT1.5-D (Figure 4D & E). Furthermore, TaHKT1.5-D showed almost no inward rectification, while TaHKT1.5-D_{S506R} was strongly inward rectifying (Figure 4F).

Dominant *HKT1;1-E^K* and *HKT1;1-E^R* alleles associated with Na^+ exclusion are derived from *V. riparia* and *V. berlandieri* respectively

To gain understanding of the origin of *VisHKT1;1* alleles, we sequenced *VisHKT1;1* from four *Vitis* species that make up this complex hybrid family (Figure 5A). The dominant E^K and E^R alleles are likely to be derived from *V. riparia* and *V. berlandieri* respectively. Both these accessions were homozygous for *E* alleles and thus provide ideal material for breeding new grapevine rootstocks with strong Na^+ exclusion ability. Conversely, the recessive e^K allele was found to originate from *V. champinii*, which is heterozygous for the e^K allele and a unique *E* allele. The e^R allele of 140 Ruggeri was derived from *V. rupestris*, which is also heterozygous for the e^R allele and another unique *E* allele (Figure S12).

The Na^+ exclusion ability of the four *Vitis* species was compared against the two parents and a selection of hybrids to determine if this trait behaved as predicted by their *HKT1;1* genotypes (Figure 5B). Indeed, *V. riparia* and *V. berlandieri* both display strong Na^+ exclusion, with minimal Na^+ accumulation in leaves, which agrees with their homozygous *HKT1;1-E* allelic makeup. Furthermore, *V. champinii* and *V. rupestris*, which both carry a recessive *HKT1;1-e* allele, showed a moderate degree of Na^+ accumulation, which was less than hybrids homozygous for *HKT1;1-e* alleles (HB55, HB25 and MI07-33) but greater than other heterozygous genotypes, K51-40 and 140 Ruggeri and hybrid HB76.

Ten *V. vinifera* wine grape cultivars commonly grown in Australia were assessed for their *HKT1;1* genetics by sequencing the SNPs underlying residues 534 and 537. All *V. vinifera* cultivars were homozygous for alleles encoding the Ser and Gly residues associated with dominant *VisHKT1;1-E* alleles. As predicted by their *HKT1;1* allelic makeup, these cultivars were strong Na^+-excluders, except for Shiraz which was a moderate Na^+-excluder (Figure 5B). This result suggests that *HKT1;1* is the major gene contributing to Na^+ exclusion in grapevines, and other minor loci yet to be identified may also contribute.

Discussion

The *NaE* QTL for Na^+ exclusion in grapevine contained six tightly linked *HKT* genes, which is the entire complement of *HKT* genes in the grapevine reference genome. This contrasts with cereals, where single *HKT* genes have been found within QTL for Na^+ exclusion (Ren *et al.*, 2005; Huang *et al.*, 2006; Byrt *et al.*, 2007), and tomato, where a QTL for Na^+ exclusion contained two closely linked *HKT* genes (Asins *et al.*, 2013). All six *HKT* genes within the *NaE* locus are predicted to encode class-1 HKT proteins containing Ser-Gly-Gly-Gly selectivity filters, suggesting they may have evolved by gene duplication, and are likely to be Na^+ selective (Mäser *et al.*, 2002; Waters *et al.*, 2013). Genetic and functional analyses presented here strongly indicates that *VisHKT1;1* is the gene responsible for variation in Na^+ exclusion associated with the *NaE* locus. VviHKT1;1 localised to the plasma membrane and was transcribed in cells associated with the root vasculature, suggesting that the Na^+ exclusion mechanism in *Vitis* species involves retrieval of Na^+ from root xylem vessels into surrounding cells, which is consistent with the role of HKT proteins in other plants (Munns & Tester, 2008; Horie *et al.*, 2009; Byrt *et al.*, 2014). *HKT1;3* was expressed in roots, but its function could not be determined here. The functions of grapevine *HKT1;2, HKT1;6, HKT1;7*, and *HKT1;8* remain to be characterised, however microarray data suggests they are not expressed in *V. vinifera* roots and are therefore unlikely to influence direct transfer of Na^+ into the root xylem. Whether they transport Na^+ and the tissues in which they function was beyond the scope of this study.

In other species, QTL mapping has identified allelic variants encoding HKT proteins that confer greater Na^+ exclusion or greater K^+:Na^+ ratios (Ren *et al.*, 2005; Asins *et al.*, 2013; Jaime-Pérez *et al.*, 2016). It has been suggested that SNPs within the coding region between tolerant and sensitive alleles of *OsHKT1;5* are responsible for the functional differences between HKT allelic variants (Cotsaftis *et al.*, 2011), but this has not been proven using mutagenesis and functional characterisation of the encoded proteins. Thus few specific amino acid residues have been identified within HKT proteins that are responsible for different Na^+-exclusion abilities of tolerant and sensitive lines. Here, we identified amino acid residues, 534 and 537, in VisHKT1;1 allelic variants that impart strong and weak shoot Na^+ exclusion when uncharged (Ser-534, Gly-537) and charged (Arg-534, Asp-537) respectively.

Single point mutations in plant HKT proteins have been shown previously to have functional impacts. For example, a Ser or Gly residue in the first pore-loop domain (p-loop A) determines Na^+ or K^+ permeability in HKTs from Arabidopsis, wheat, rice and Venus flytrap (*Dionaea muscipula*) (Mäser *et al.*, 2002; Böhm *et al.*, 2016). Mutation of an Asp to Asn in the second p-loop domain of *Thellungiella salsuginea* TsHKT1;2 and the Arabidopsis ortholog (to create TsHKT1;2_{D207N} and *AtHKT1*$_{N211D}$) altered their Na^+/K^+ selectivity, and expression of TsHKT1;2 or the mutant Arabidopsis protein conferred greater salt tolerance to Arabidopsis *hkt1 -1* knockout plants due to increased K^+ accumulation in shoots (Ali *et al.*, 2012). In our study, the VisHKT1;1-e proteins had identical cation selectivity to VisHKT1;1-E variants, suggesting that the increased Na^+ transport activity of VisHKT1;1-E variants confers the mechanism for improved Na^+ exclusion in *NaE* progeny.

HKT proteins from rice that display strong (OsHKT1;1) and weak (OsHKT1;3) inward rectification have been observed (Jabnoune *et al.*, 2009). We identified a single amino acid residue (Arg-534) that caused greater inward rectification of VisHKT1;1-e variants compared to VisHKT1;1-E variants. We found that mutating the corresponding residue in wheat TaHKT1.5-D also caused inward rectification and reduced Na^+ conductance. Both rice OsHKT1;1 and 1;3 appear to rectify more strongly than VisHKT1;1-e and wheat TaHKT1.5-D_{S506R}, and neither contain a residue equivalent to Arg-534. TsHKT1;2 and AtHKT1$_{N211D}$ showed inward rectification of Na^+ transport, but the reverse D207N mutation in TsHKT1;2 did not abrogate this (Ali *et al.*, 2016). These findings indicate that additional residues influence rectification in HKT proteins.

Ali *et al.* (2016) suggested that inward rectification of AtHKT1;1^{N211D} would impose a greater Na^+ retention in root cells, preventing Na^+ efflux to the xylem apoplast. However, they found no difference in shoot Na^+ accumulation between Arabidopsis plants expressing either the rectifying or non-rectifying AtHKT1 variants. In contrast, in our study, inheritance of the non-inwardly rectifying VisHKT1;1-E alleles correlated with greater shoot Na^+ exclusion. Therefore, the greater Na^+ conductance observed through the HKT1 variants at physiologically relevant membrane potentials is likely to be the major contributing factor to shoot Na^+ exclusion. This aligns with the suggestion by Ren *et al.* (2005) that the rice *SKC1* allelic variant from salt tolerant variety Nona Bokra shows greater Na^+ conductance than the allele from salt sensitive Koshihikari. It also agrees with thermodynamics of Na^+ transport in

root xylem parenchyma cells, which is predicted to be inward (to the cytoplasm) through channel-like proteins such as HKT, and outward (towards to xylem apoplast) through secondary active Na^+/H^+ exchangers (Munns & Tester, 2008). The functional role of inward rectification of plant HKT proteins therefore remains unclear. However, it must be noted that a greater degree of rectification was correlated with a lower magnitude of Na^+ current at negative potentials in all the HKT variants and mutants studied here, so the two properties are likely to be linked.

In our study, the R534S mutation in VisHKT1;1-e^K reduced inward rectification and increased inward Na^+ conductance. Within physiological pH ranges, the side chain of Arg-534 in VisHKT1;1-e^K is expected to be positively charged. The importance of positively charged residues in the $M2_D$ region of Trk/Ktr/HKT proteins has previously been demonstrated for AtHKT1 and TaHKT2;1 – mutation of Arg-519 in TaHKT2;1 and the equivalent Arg-487 in AtHKT1 to uncharged Gln reduced the transport activity of both proteins (Kato *et al.*, 2007). In contrast, we found that replacing the charged residues in the $M2_D$ region with uncharged residues increased the activity of VisHKT1;1-e^K. The additive effect of a D537G substitution on transport activity in the VisHKT1;1-$e^K_{R534S/D537G}$ double mutant protein in yeast, but no change in conductance of the VisHKT1;1-e^K_{D537G} single mutant, might be due to interactions between positive and negative side chains of the Arg-534 and Asp-537 residues in original VisHKT1;1-e^K. Future structural investigations into plant HKT proteins through protein crystallisation would help to explain these observations. In the parental rootstocks, expression of recessive *VisHKT1;1-e* alleles was approximately 2-fold less than the dominant *VisHKT1;1-E* alleles in the root stele. The F1 progeny are likely to have similar expression levels of each allele. Arabidopsis double knockout mutants of two transcription factors *arr1/arr12* showed a 6-fold increase in *AtHKT1* expression in roots, which correlated with a 50% reduction in shoot Na^+ concentration (Mason *et al.*, 2010). A 2-fold increase in transcript abundance of allele *E* variants over allele *e* is therefore probably not large enough to explain the large difference in leaf Na^+ that we observed between the homozygous *NaE* and *Nae* hybrid progeny. While expression differences may contribute to leaf Na^+ exclusion, functional differences in Na^+ transport are likely the major determining factor for the near-Mendelian inheritance of Na^+ exclusion seen in our study.

Ten *V. vinifera* cultivars examined here, were all homozygous for *VvHKT1;1* alleles encoding Ser and Gly residues at 534 and 537 – typical of dominant *VisHKT1;1-E* alleles. The majority of these cultivars showed strong Na^+ exclusion abilities consistent with their *HKT1;1* alleles. This finding highlights the importance of selecting for dominant *VisHKT1;1-E* alleles in new rootstock genotypes, as introducing recessive *VisHKT1;1-e* alleles could result in severely diminished Na^+ exclusion capability compared with own-rooted *V. vinifera*.

In plants, both Na^+ and Cl^- can be toxic in high enough concentrations (Tavakkoli *et al.*, 2011), and which ion is more damaging depends on both their relative accumulation and thresholds of toxicity (Munns & Tester, 2008). In grapevines, Cl^- has been attributed as the ion most associated with salinity related ion toxicity; however, early studies that established this link were limited to *V. vinifera* cultivars (Woodham, 1956; Ehlig, 1960; Downton, 1977b). In our study, all the *V. vinifera* cultivars were found to be relatively strong excluders of Na^+. Considering Na^+ exclusion is much more variable in rootstock genotypes derived from other *Vitis* species and the prevalent use of rootstocks in viticulture, the impact of elevated Na^+ accumulation on vine health warrants further investigation. The homozygous recessive *Nae* hybrids identified here provide the ideal rootstock material for quantifying the effect of high Na^+ accumulation on vine health and yield in longer-term future studies.

In conclusion, we identified *VisHKT1;1* as a major gene controlling Na^+ exclusion in grapevine rootstocks. Transgressive variation of Na^+ exclusion in the progeny of a heterozygous rootstock cross is caused by the inheritance of *VisHKT1;1* alleles that encode proteins with differences in Na^+ conductance, voltage dependence, and have small differences in root expression levels. We propose that the mechanism for enhanced Na^+ exclusion in *NaE* progeny is the enhanced Na^+ conductance through VisHKT1;1-E variants, which also display limited rectification. These functional properties are conferred by a neutrally charged amino acid residue at the C-terminus of VisHKT1;1. Identification of dominant *VisHKT1;1-E* alleles provide a valuable genetic marker to select for strong Na^+ exclusion in rootstock breeding programs, which will assist with quality grape and wine production from saline soils.

Acknowledgements

We thank Diversity Array Technology (ACT) for GBS. Bettina Berger and Plant Accelerator staff (Waite Campus), Annette Böttcher, Karin Sefton, Amy Rinaldo, Jim Speirs, Caroline Phillips, Alex Lawlor, Maria Mrinak, Inna Mazonka, Charlotte Jordans, Matthew Woodward and Simon Robinson (CSIRO) for assistance with Na^+ screening. CSIRO Analytical Services Unit for ICP. Peter Clingeleffer and Arryn Clarke (CSIRO) for maintaining rootstock mothervines. Haijun Gong, Lauren Hooper and Jacinta Watkins (CSIRO) for assistance with sequencing and cloning. Paul Boss (CSIRO) for assistance with QTL mapping. Wendy Sullivan (University of Adelaide) for technical assistance. Stefanie Wege (University of Adelaide) for microscopy assistance. Bo Xu (University of Adelaide) for TaHKT1;5-D in pGEMHE. Maria Hrmova (University of Adelaide) for discussions on experimental design. Steve Tyerman (University of Adelaide) for assistance with data analysis. This work was funded by Wine Australia grant CSP1302 (A.R.W, R.R.W, E.J.E, M.G.) with support from ARC grants FT130100709 and CE140100008 (both M.G.), Department of Agriculture and Water Resources Science and Innovation Award (J.D.D.), and AGW_Ph1502 (Y.W).

Author contributions

S.W.H performed yeast assays, qRT-PCR, cloning, confocal microscopy, site-directed mutagenesis, and electrophysiology of grapevine HKT variants. J.D.D performed linkage mapping, QTL analysis, primer design, cloning of HKT1;1 allelic variants, and sequencing of HKT1;1 from *Vitis* species. Y.W. performed mutagenesis and electrophysiology of TaHKT1;5-D. A.R.W, E.J.E, R.R.W, D.H.B, and J.D.D, devised and performed grapevine Na^+ screens and D.H.B measured the leaf Na^+ content. S.W.H. and J.D.D analysed data. M.G, R.R.W and A.R.W supervised research. S.W.H. and J.D.D wrote the manuscript. M.G., R.R.W. and A.R.W. revised the manuscript. All authors commented on the manuscript.

References

Ali A, Raddatz N, Aman R, Kim S, Park HC, Jan M, Baek D, Khan IU, Oh D-H, Lee SY, et al. 2016. A single amino-acid substitution in the sodium transporter HKT1 associated with plant salt tolerance. *Plant Physiology* **171**: 2112-2126.

Ali Z, Park HC, Ali A, Oh D-H, Aman R, Kropornicka A, Hong H, Choi W, Chung WS, Kim W-Y, et al. 2012. TsHKT1;2, a HKT1 homolog from the extremophile *Arabidopsis* relative *Thellungiella salsuginea*, shows K^+ specificity in the presence of NaCl. *Plant Physiology* **158**: 1463-1474.

Asins MJ, Villalta I, Aly MM, Olías R, Álvarez De Morales PAZ, Huertas R, Li JUN, Jaime-Pérez N, Haro R, Raga V, et al. 2013. Two closely linked tomato HKT coding genes are positional candidates for the major tomato QTL involved in Na^+/K^+ homeostasis. *Plant, Cell & Environment* **36**: 1171-1191.

Baxter I, Brazelton JN, Yu D, Huang YS, Lahner B, Yakubova E, Li Y, Bergelson J, Borevitz JO, Nordborg M, et al. 2010. A coastal cline in sodium accumulation in *Arabidopsis thaliana* is driven by natural variation of the sodium transporter AtHKT1;1. *PLOS Genetics* **6**: e1001193.

Benheim D, Rochfort S, Robertson E, Potter ID, Powell KS. 2012. Grape phylloxera (*Daktulosphaira vitifoliae*) – a review of potential detection and alternative management options. *Annals of Applied Biology* **161**: 91-115.

Böhm J, Scherzer S, Shabala S, Krol E, Neher E, Mueller TD, Hedrich R. 2016. Venus flytrap HKT1-type channel provides for prey sodium uptake into carnivorous plant without conflicting with electrical excitability. *Molecular Plant* **9**: 428-436.

Byrt CS, Platten JD, Spielmeyer W, James RA, Lagudah ES, Dennis ES, Tester M, Munns R. 2007. HKT1;5-like cation transporters linked to Na^+ exclusion loci in wheat, *Nax2* and *Kna1*. *Plant Physiology* **143**: 1918-1928.

Byrt CS, Xu B, Krishnan M, Lightfoot DJ, Athman A, Jacobs AK, Watson-Haigh NS, Plett D, Munns R, Tester M, et al. 2014. The Na^+ transporter, TaHKT1;5-D, limits shoot Na^+ accumulation in bread wheat. *The Plant Journal* **80**: 516-526.

Corratgé-Faillie C, Jabnoune M, Zimmermann S, Véry A-A, Fizames C, Sentenac H. 2010. Potassium and sodium transport in non-animal cells: the Trk/Ktr/HKT transporter family. *Cellular and Molecular Life Sciences* **67**: 2511-2532.

Cotsaftis O, Plett D, Johnson AAT, Walia H, Wilson C, Ismail AM, Close TJ, Tester M, Baumann U. 2011. Root-specific transcript profiling of contrasting rice genotypes in response to salinity stress. *Molecular Plant* **4**: 25-41.

Cotsaftis O, Plett D, Shirley N, Tester M, Hrmova M. 2012. A two-staged model of Na^+ exclusion in rice explained by 3D modeling of HKT transporters and alternative splicing. *Plos One* **7**: e39865.

Courtois B, Audebert A, Dardou A, Roques S, Ghneim- Herrera T, Droc G, Frouin J, Rouan L, Gozé E, Kilian A, et al. 2013. Genome-wide association mapping of root traits in a japonica rice panel. *Plos One* **8**: e78037.

Curtis MD, Grossniklaus U. 2003. A gateway cloning vector set for high-throughput functional analysis of genes in planta. *Plant Physiology* **133**: 462-469.

Davenport RJ, Munoz-Mayor A, Jha D, Essah PA, Rus ANA, Tester M. 2007. The Na^+ transporter AtHKT1;1 controls retrieval of Na^+ from the xylem in *Arabidopsis*. *Plant, Cell & Environment* **30**: 497-507.

de Loryn LC, Petrie PR, Hasted AM, Johnson TE, Collins C, Bastian SEP. 2014. Evaluation of sensory thresholds and perception of sodium chloride in grape juice and wine. *American Journal of Enology and Viticulture* **65**: 124-133.

Donkin R, Robinson S, Sumby K, Harris V, McBryde C, Jiranek V. 2010. Sodium chloride in Australian grape juice and its effect on alcoholic and malolactic fermentation. *American Journal of Enology and Viticulture* **61**: 392-400.

Downton WJS. 1977a. Chloride accumulation in different species of grapevine. *Scientia Horticulturae* **7**: 249-253.

Downton WJS. 1977b. Photosynthesis in salt-stressed grapevines. *Australian Journal of Plant Physiology* **4**: 183-192.

Ehlig CF. 1960. Effects of salinity on four varieties of table grapes grown in sand culture. *Proceedings of the American Society for Horticultural Sciences* **76**: 323-331.

Elliott J, Deryng D, Müller C, Frieler K, Konzmann M, Gerten D, Glotter M, Flörke M, Wada Y, Best N, et al. 2014. Constraints and potentials of future irrigation water availability on agricultural production under climate change. *Proceedings of the National Academy of Sciences* **111**: 3239-3244.

Fasoli M, Dal Santo S, Zenoni S, Tornielli GB, Farina L, Zamboni A, Porceddu A, Venturini L, Bicego M, Murino V, et al. 2012. The grapevine expression atlas reveals a deep transcriptome shift driving the entire plant into a maturation program. *The Plant Cell Online* **24**: 3489-3505.

Ferris H, Zheng L, Walker MA. 2012. Resistance of grape rootstocks to plant-parasitic nematodes. *Journal of Nematology* **44**: 377-386.

Fort KP, Heinitz CC, Walker MA. 2015. Chloride exclusion patterns in six grapevine populations. *Australian Journal of Grape and Wine Research* **21**: 147-155.

Gong H, Blackmore D, Clingeleffer P, Sykes S, Jha D, Tester M, Walker R. 2011. Contrast in chloride exclusion between two grapevine genotypes and its variation in their hybrid progeny. *Journal of Experimental Botany* **62**: 989-999.

Gong HJ, Blackmore DH, Clingeleffer PR, Sykes SR, Walker RR. 2014. Variation for potassium and sodium accumulation in a family from a cross between grapevine rootstocks K 51-40 and 140 Ruggeri. *Vitis* **53**: 65–72.

Grefen C, Donald N, Hashimoto K, Kudla J, Schumacher K, Blatt MR. 2010. A ubiquitin-10 promoter-based vector set for fluorescent protein tagging facilitates temporal stability and native protein distribution in transient and stable expression studies. *The Plant Journal* **64**: 355-365.

Henderson SW, Baumann U, Blackmore DH, Walker AR, Walker RR, Gilliham M. 2014. Shoot chloride exclusion and salt tolerance in grapevine is associated with differential ion transporter expression in roots. *BMC Plant Biology* **14**: 1-18.

Henderson SW, Wege S, Qiu J, Blackmore DH, Walker AR, Tyerman SD, Walker RR, Gilliham M. 2015. Grapevine and Arabidopsis cation-chloride cotransporters localize to the Golgi and *trans*-Golgi network and indirectly influence long-distance ion transport and plant salt tolerance. *Plant Physiology* **169**: 2215-2229.

Horie T, Hauser F, Schroeder JI. 2009. HKT transporter-mediated salinity resistance mechanisms in Arabidopsis and monocot crop plants. *Trends in Plant Science* **14**: 660-668.

Huang S, Spielmeyer W, Lagudah ES, James RA, Platten JD, Dennis ES, Munns R. 2006. A sodium transporter (HKT7) is a candidate for *Nax1*, a gene for salt tolerance in durum wheat. *Plant Physiology* **142**: 1718-1727.

Jabnoune M, Espeout S, Mieulet D, Fizames C, Verdeil J-L, Conéjéro G, Rodríguez-Navarro A, Sentenac H, Guiderdoni E, Abdelly C, et al. 2009. Diversity in expression patterns and functional properties in the rice HKT transporter family. *Plant Physiology* **150**: 1955-1971.

Jaillon O, Aury JM, Noel B, Policriti A, Clepet C, Casagrande A, Choisne N, Aubourg S, Vitulo N, Jubin C, et al. 2007. The grapevine genome sequence suggests ancestral hexaploidization in major angiosperm phyla. *Nature* **449**: 463-U465.

Jaime-Pérez N, Pineda B, García-Sogo B, Atares A, Athman A, Byrt CS, Olías R, Asins MJ, Gilliham M, Moreno V, et al. 2016. The Na^+ transporter encoded by the HKT1;2 gene modulates Na^+/K^+ homeostasis in tomato shoots under salinity. *Plant, Cell & Environment* **40**: 658–671.

James RA, Blake C, Byrt CS, Munns R. 2011. Major genes for Na^+ exclusion, *Nax1* and *Nax2* (wheat *HKT1;4* and *HKT1;5*), decrease Na^+ accumulation in bread wheat leaves under saline and waterlogged conditions. *Journal of Experimental Botany* **62**: 2939-2947.

Kato N, Akai M, Zulkifli L, Matsuda N, Kato Y, Goshima S, Hazama A, Yamagami M, Guy RH, Uozumi N. 2007. Role of positively charged amino acids in the M2D transmembrane helix of Ktr/Trk/HKT type cation transporters. *Channels* **1**: 161-171.

Leske PA, Sas AN, Coulter AD, Stockley CS, Lee TH. 1997. The composition of Australian grape juice: chloride, sodium and sulfate ions. *Australian Journal of Grape and Wine Research* **3**: 26-30.

Li B, Tester M, Gilliham M. 2017. Chloride on the move. *Trends in Plant Science* **22**: 236-248.

Li X-L, Wang C-R, Li X-Y, Yao Y-X, Hao Y-J. 2013. Modifications of Kyoho grape berry quality under long-term NaCl treatment. *Food Chemistry* **139**: 931-937.

Maas EV, Hoffman GJ. 1977. Crop salt tolerance - current assessment. *Journal of the Irrigation and Drainage Division* **103**: 115-134.

Mäser P, Hosoo Y, Goshima S, Horie T, Eckelman B, Yamada K, Yoshida K, Bakker EP, Shinmyo A, Oiki S, et al. 2002. Glycine residues in potassium channel-like selectivity filters determine potassium selectivity in four-loop-per-subunit HKT transporters from plants. *Proceedings of the National Academy of Sciences* **99**: 6428-6433.

Mason MG, Jha D, Salt DE, Tester M, Hill K, Kieber JJ, Eric Schaller G. 2010. Type-B response regulators ARR1 and ARR12 regulate expression of AtHKT1;1 and accumulation of sodium in Arabidopsis shoots. *The Plant Journal* **64**: 753-763.

Møller IS, Gilliham M, Jha D, Mayo GM, Roy SJ, Coates JC, Haseloff J, Tester M. 2009. Shoot Na^+ exclusion and increased salinity tolerance engineered by cell type-specific alteration of Na^+ transport in *Arabidopsis*. *Plant Cell* **21**: 2163-2178.

Munns R, Gilliham M. 2015. Salinity tolerance of crops – what is the cost? *New Phytologist* **208**: 668–673.

Munns R, James RA, Xu B, Athman A, Conn SJ, Jordans C, Byrt CS, Hare RA, Tyerman SD, Tester M, et al. 2012. Wheat grain yield on saline soils is improved by an ancestral Na^+ transporter gene. *Nature Biotechnology* **30**: 360-364.

Munns R, Tester M. 2008. Mechanisms of salinity tolerance. *Annual Review of Plant Biology* **59**: 651-681.

Nelson BK, Cai X, Nebenführ A. 2007. A multicolored set of *in vivo* organelle markers for co-localization studies in Arabidopsis and other plants. *The Plant Journal* **51**: 1126-1136.

Ollat N, Bordenave L, Tandonnet JP, Boursiquot JM, Marguerit E 2016. Grapevine rootstocks: origins and perspectives: International Society for Horticultural Science (ISHS), Leuven, Belgium. 11-22.

Pannell DJ. 2001. Dryland salinity: economic, scientific, social and policy dimensions. *Australian Journal of Agricultural and Resource Economics* **45**: 517-546.

Prior LD, Grieve AM, Cullis BR. 1992. Sodium-chloride and soil texture interactions in irrigated field-grown sultana grapevines. I. Yield and fruit-quality. *Australian Journal of Agricultural Research* **43**: 1051-1066.

Ren Z-H, Gao J-P, Li L-G, Cai X-L, Huang W, Chao D-Y, Zhu M-Z, Wang Z-Y, Luan S, Lin H-X. 2005. A rice quantitative trait locus for salt tolerance encodes a sodium transporter. *Nature Genetics* **37**: 1141-1146.

Rus A, Baxter I, Muthukumar B, Gustin J, Lahner B, Yakubova E, Salt DE. 2006. Natural variants of AtHKT1 enhance Na^+ accumulation in two wild populations of Arabidopsis. *PLOS Genetics* **2**: e210.

Sainsbury F, Thuenemann EC, Lomonossoff GP. 2009. pEAQ: versatile expression vectors for easy and quick transient expression of heterologous proteins in plants. *Plant Biotechnology Journal* **7**: 682-693.

Serra I, Strever A, Myburgh PA, Deloire A. 2014. Review: the interaction between rootstocks and cultivars (*Vitis vinifera* L.) to enhance drought tolerance in grapevine. *Australian Journal of Grape and Wine Research* **20**: 1-14.

Stevens RM, Harvey G, Partington DL. 2011. Irrigation of grapevines with saline water at different growth stages: effects on leaf, wood and juice composition. *Australian Journal of Grape and Wine Research* **17**: 239-248.

Stevenson I. 1980. The diffusion of disaster: The phylloxera outbreak in the département of the Hérault, 1862–1880. *Journal of Historical Geography* **6**: 47-63.

Stockley CS, Lloyd-Davies S. 2001. *Analytical specifications for the export of Australian wine: a list of analysis requirements and specifications for Australian wine export destinations.* Glen Osmond, S.A: The Australian Wine Research Institute.

Sunarpi, Horie T, Motoda J, Kubo M, Yang H, Yoda K, Horie R, Chan W-Y, Leung H-Y, Hattori K, et al. 2005. Enhanced salt tolerance mediated by AtHKT1 transporter-induced Na^+ unloading from xylem vessels to xylem parenchyma cells. *The Plant Journal* **44**: 928-938.

Tavakkoli E, Fatehi F, Coventry S, Rengasamy P, McDonald GK. 2011. Additive effects of Na^+ and Cl^- ions on barley growth under salinity stress. *Journal of Experimental Botany* **62**: 2189-2203.

Tounsi S, Ben Amar S, Masmoudi K, Sentenac H, Brini F, Véry A-A. 2016. Characterization of two HKT1;4 transporters from *Triticum monococcum* to elucidate the determinants of the wheat salt tolerance *Nax1* QTL. *Plant and Cell Physiology* **57**: 2047-2057.

Tregeagle JM, Tisdall JM, Tester M, Walker RR. 2010. Cl^- uptake, transport and accumulation in grapevine rootstocks of differing capacity for Cl^- exclusion. *Functional Plant Biology* **37**: 665-673.

Van Ooijen J. 2006. JoinMap® 4, Software for the calculation of genetic linkage maps in experimental populations. *Kyazma BV, Wageningen* **33**: 10.1371.

Van Ooijen J, Kyazma B. 2009. MapQTL 6. *Software for the mapping of quantitative trait loci in experimental populations of diploid species. Kyazma BV: Wageningen, Netherlands.*

Walker RR, Blackmore DH, Clingeleffer PR, Correll RL. 2002. Rootstock effects on salt tolerance of irrigated field-grown grapevines (*Vitis vinifera* L. cv. Sultana). 1. Yield and vigour inter-relationships. *Australian Journal of Grape and Wine Research* **8**: 3-14.

Walker RR, Blackmore DH, Clingeleffer PR, Correll RL. 2004. Rootstock effects on salt tolerance of irrigated field-grown grapevines (*Vitis vinifera* L. cv. Sultana) 2. Ion concentrations in leaves and juice. *Australian Journal of Grape and Wine Research* **10**: 90-99.

Walker RR, Blackmore DH, Clingeleffer PR, Godden P, Francis L, Valente P, Robinson E. 2003. Salinity effects on vines and wines. *Bulletin de l'Office. International de la Vigne et du Vin* **76**: 200-227.

Waters S, Gilliham M, Hrmova M. 2013. Plant high-affinity potassium (HKT) transporters involved in salinity tolerance: structural insights to probe differences in ion selectivity. *International Journal of Molecular Sciences* **14**: 7660.

Woodham R. 1956. The chloride status of the irrigated sultana vine and its relation to vine health. *Australian Journal of Agricultural Research* **7**: 414-427.

Supporting Information

Figure Legends

Figure 1 Na^+ exclusion is associated with a major QTL on chromosome 11 which contains a cluster of six *HKT1* genes

(A) Leaf Na^+ concentration in a population of K51-40 x 140 Ruggeri hybrids. The parents K51-40 and 140 Ruggeri are indicated in black. Hybrid progeny are coloured according to their inheritance of SNP markers at 13.7 Mb within the *NaE* locus. Hybrids homozygous for the dominant *NaE* locus are indicated in yellow and progeny homozygous for recessive *nae* locus are indicated in red. Progeny heterozygous for a dominant NaE^K locus from K51-40 and a recessive nae^R locus from 140 Ruggeri are indicated in mustard, while progeny heterozygous for a recessive nae^K locus from K51-40 and dominant NaE^R locus from 140 Ruggeri are indicated in orange. Bars are mean + SEM of 3 biological replicates. (B) Schematic of chromosome 11 Na^+ exclusion QTL mapping interval, shows map units in cM (left) and the physical position of SNPs in Mb corresponding to the grapevine reference sequence (right). Vertical dashed line represents the genome-wide significance threshold *P* value of 0.01. (C) Relative positions of *HKT1* genes (black arrows) on part of chromosome 11 based on the grapevine reference genome. *VviHKT1;1* (VIT_211s0103g00010), *VviHKT1;3* (VIT_211s0103g00050), *VviHKT1;2* (VIT_211s0103g00090), *VviHKT1;8* (VIT_211s0103g00130), *VviHKT1;7* (VIT_211s0103g00140), *VviHKT1;6* (VIT_211s0103g00150). White arrows signify unrelated genes. Not to scale.

Figure 2: HKT1;1 is a functional Na^+ transporter on the plasma membrane of grapevine root stelar cells.

(A) Expression level of *HKT* transcripts in *V. vinifera* roots determined by microarray hybridisation. Each point represents a unique probe from the microarray. Data are mean ± SEM of three biological replicates. Data are from Fasoli *et al*. (2012). (B) Current-voltage relationship of *X. laevis* oocytes injected with water (red diamonds) *VviHKT1;3* (black squares) or *VviHKT1;1* (blue circles). Oocytes were clamped from +60 to -140 mV in a solution containing 10 mM Na^+-gluconate, pH 5.5. Data are mean ± SEM (n = 3 oocytes). (C) Relative *HKT1;1* transcript abundance in root tissue enriched in epidermal and stelar (dark blue bars) or epidermal/cortical cells (light blue bars) from grapevine rootstocks K51-40 and

140 Ruggeri. Data are means ± SEM of three biological replicates of pooled tissue from multiple plants. Data are relative to the K51-40 stelar replicate with the greatest transcript abundance. Asterisk denotes significant difference between tissue types ($P < 0.05$; Student's t test). (D) Tobacco (*N. benthamina*) leaf epidermal cells expressing VviHKT1;1-GFP (upper panels), free GFP (middle panels), or VviHKT1;1-GFP plus the ER marker HDEL-mCherry (lower panels). Leaves in the upper and middle panels were imaged 10 mins after infiltration with FM4-46, which predominantly stained the plasma membrane. Leaves were imaged by confocal microscopy 2 days after agroinfiltration. Scale bar = 10 µm. (E) Signal profiles of GFP (green) and FM4-64 or mCherry (magenta) corresponding to the arrow in the adjacent merged image from D. Overlapping peaks indicate colocalisation between the two signals.

Figure 3: Grapevine rootstock *VisHKT1;1* allelic variants have different expression, and Na^+ transport properties.

(A) Amino acid alignment of *V. vinifera* HKT1;1 from Cabernet Sauvignon with protein sequences predicted from unique alleles of *VisHKT1;1* present in K51-40 (E^K and e^K) and 140 Ruggeri (E^R and e^R). Residues conserved in three or more sequences are shown in black with unique residues encoded by a single allele shown in grey. Encoded residue conserved between E allele are highlighted in yellow and those conserved between e alleles are highlighted in red. Predicted transmembrane regions ($M1_{A-D}$ & $M2_{A-D}$), and P-loop domains (P_{A-D}) are shown above. Arrows indicate the position of residues in the selectivity filter. Asterisks indicate residues selected for mutagenesis. (B) Copy number of mRNAs encoding different *VisHKT1;1* alleles in root tissue enriched stelar or epidermal/cortical cells from grapevine rootstocks K51-40 (left) and 140 Ruggeri (right). Data are means ± SEM of three biological replicates of pooled tissue from multiple plants. Significant differences are denoted by different letters ($P < 0.05$, one-way ANOVA with Tukey's post-hoc test). (C) VisHKT1;1 allelic variants differentially inhibit yeast growth on high Na^+. Wild-type strain INVSc2 was transformed with pYES-DEST52 empty vector as a control, or the same vector containing allelic variants of VisHKT1;1. Diluted yeast strains were spotted (5 µL) onto plates containing D-glucose (spotting control), or D-raffinose and D-galactose (induction) ± 50 mM NaCl. Plates were incubated at 30 °C for 3 days. (D) Typical currents observed from oocytes injected with cRNA encoding VisHKT1;1-E^K, VisHKT1;1-e^K, VisHKT1;1-E^R, VisHKT1;1-e^R, and water, in solutions containing 30 mM Na^+-gluconate. Dashed lines represent zero current

levels. Data represent total oocyte currents without background subtraction. Data are mean ± SEM (n ≥ 5 oocytes).

Figure 4: Arg-534 and Asp-537 control the gating and sodium conductance of VisHKT1;1-e^{K}.

(A) Normalised current-voltage relationships of oocytes injected with water or cRNA encoding VisHKT1;1-e^{K}, VisHKT1;1-e$^{K}_{D537G}$, VisHKT1;1-e$^{K}_{R534S}$, and VisHKT1;1-e$^{K}_{R534S/D537G}$ in solutions with 30 mM Na^+-gluconate. Data represent the HKT-mediated currents without background subtraction. Data are mean ± SEM (n ≥ 9 oocytes from 2 batches). (B) The inward chord conductance (G_{Na+}) ratio of Xenopus oocytes expressing VisHKT1;1-e^{K} and mutated variants in solutions containing 30 mM Na^+-gluconate. The rectification ratio was determined by dividing G_{Na+} at -140 mV by G_{Na+} at +60 mV. Chord conductances were calculated from current-voltage relationships using the equation $G_{Na+} = I / (V_m - V_{rev})$. Data are mean ± SEM (n ≥ 5 oocytes) and calculations were performed after subtraction of mean background currents from water injected control oocytes. Asterisk denotes significant difference from wild-type (t-test, $P < 0.05$). (C) Comparison of Na^+-induced growth inhibition of INVSc2 yeast strains expressing wild-type and mutant *VisHKT1;1* alleles from K51-40. Yeast were spotted onto plates containing D-glucose (control), or D-raffinose and D-galactose (induction) ± 50 mM NaCl. Plates were incubated at 30 °C for 2 days (glucose) or 4 days (galactose). (D-E) Current-voltage relationships of oocytes injected with cRNA encoding TaHKT1;5-D (D) and TaHKT1;5-D$_{S506R}$ (E) in solutions with 30 mM Na^+-gluconate. Data represent the HKT-mediated currents after background subtraction. Data are mean ± SEM (n ≥ 9 oocytes). (F) The inward chord conductance (G_{Na+}) ratio of Xenopus oocytes expressing TaHKT1;5-D and TaHKT1;5-D$_{S506R}$ in solutions containing 30 mM Na^+-gluconate. Data are mean ± SEM (n ≥ 9 oocytes). Asterisk denotes significant difference from wild-type (t-test, $P < 0.01$).

Figure 5: Recessive alleles, *VisHKT1;1*-e^{K} and *VisHKT1;1*-e^{R}, are derived from *V. champinii* and *V. rupestris* respectively.

(A) Pedigree diagram of K51-40 and 140 Ruggeri illustrating the inheritance of *VisHKT1;1* alleles from four different grandparent *Vitis* species. *V. champinii* and *V. rupestris* are heterozygous carriers of the recessive *VisHKT1;1-e^{K}* and *VisHKT1;1-e^{R}* allele respectively,

while *V. riparia* and *V. berlandieri* appear to be homozygous for the dominant *VisHKT1;1*-E^K and *VisHKT1;*1-E^R alleles respectively. (B) Na^+ exclusion in selected progeny of K51-40 x 140 Ruggeri (from Figure 1A), the parents and grandparents, and *V. vinifera* cultivars. Individuals are coloured according to their deduced amino acids at the key residues 534 and 537 of VisHKT1;1 as determined by direct genomic DNA sequencing (Figure S12). Yellow bars indicate genotypes homozygous for the dominant *HKT1;1-E* alleles (residues Ser-534 and Gly-537). Red bars indicate genotypes homozygous for the recessive *HKT1;1-e* alleles (residues Arg-534 and Asp-537), and orange bars indicate heterozygous genotypes that contain one dominant *HKT1;1-E* allele and one recessive *HKT1;1-e* allele. Bars are mean + SEM of 3 biological replicates. Significant differences are denoted by different letters ($P < 0.05$, one-way ANOVA with Tukey's post-hoc test.

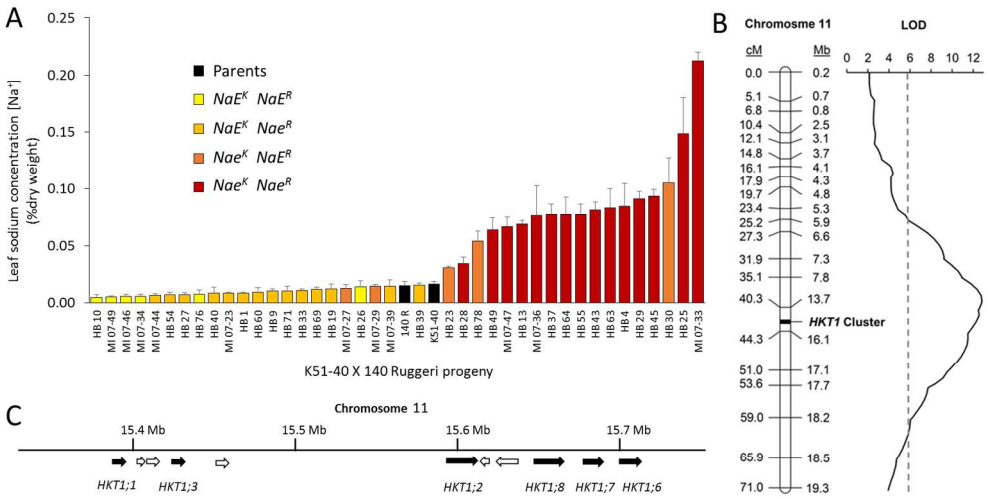

Figure 1 Na+ exclusion is associated with a major QTL on chromosome 11 which contains a cluster of six HKT1 genes.

338x190mm (300 x 300 DPI)

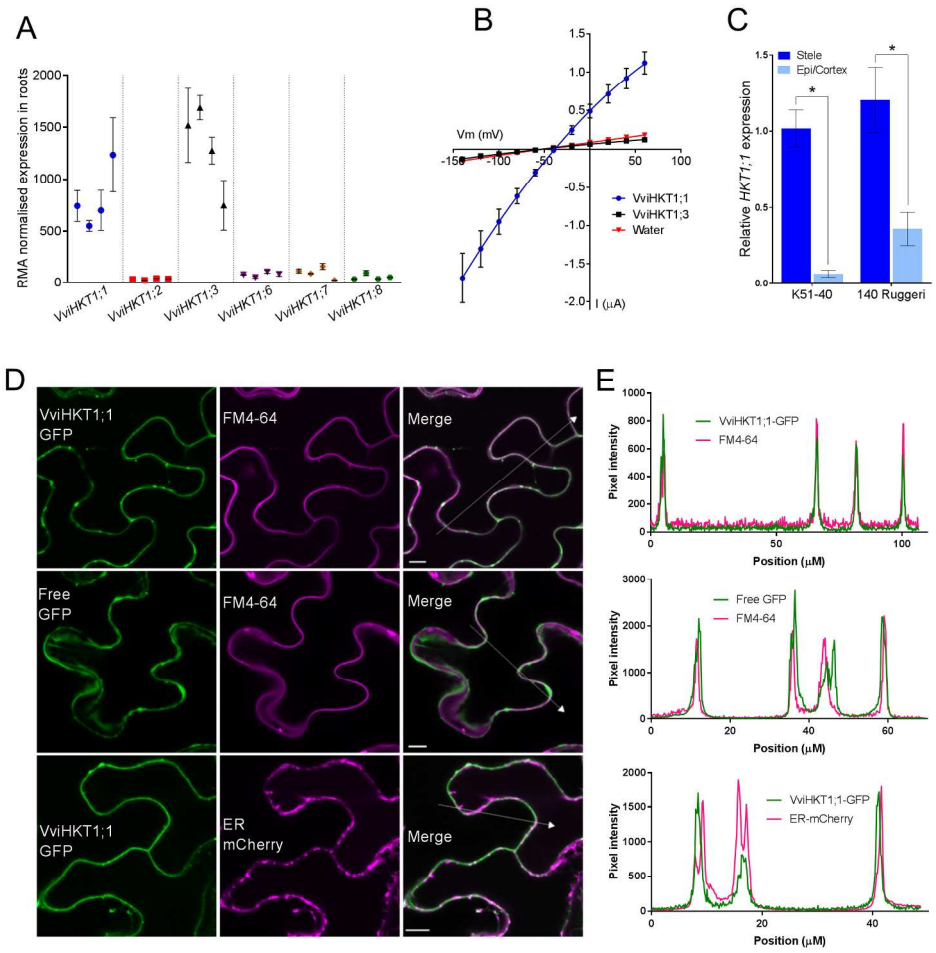

Figure 2: HKT1;1 is a functional Na+ transporter on the plasma membrane of grapevine root stelar cells.

204x202mm (300 x 300 DPI)

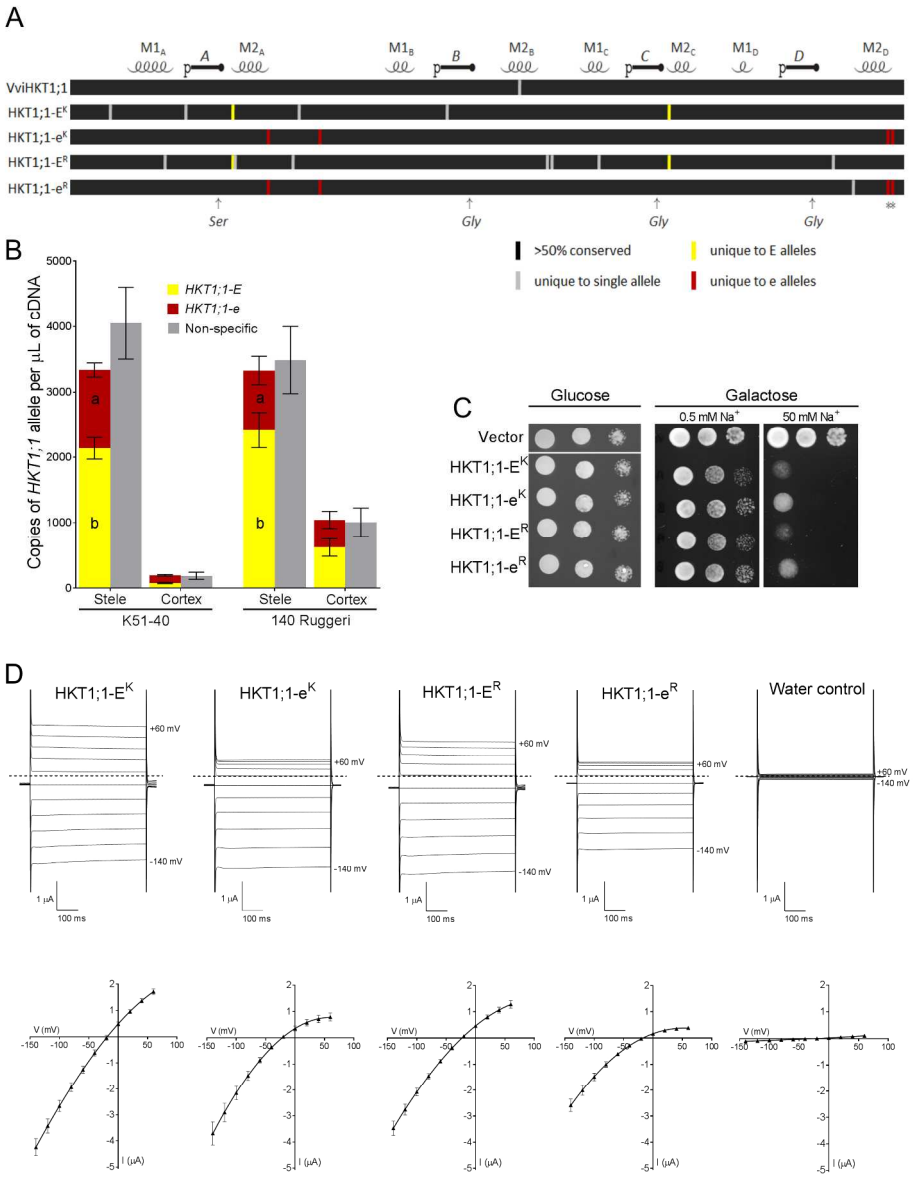

Figure 3: Grapevine rootstock VisHKT1;1 allelic variants have different expression, and Na+ transport properties.

213x277mm (300 x 300 DPI)

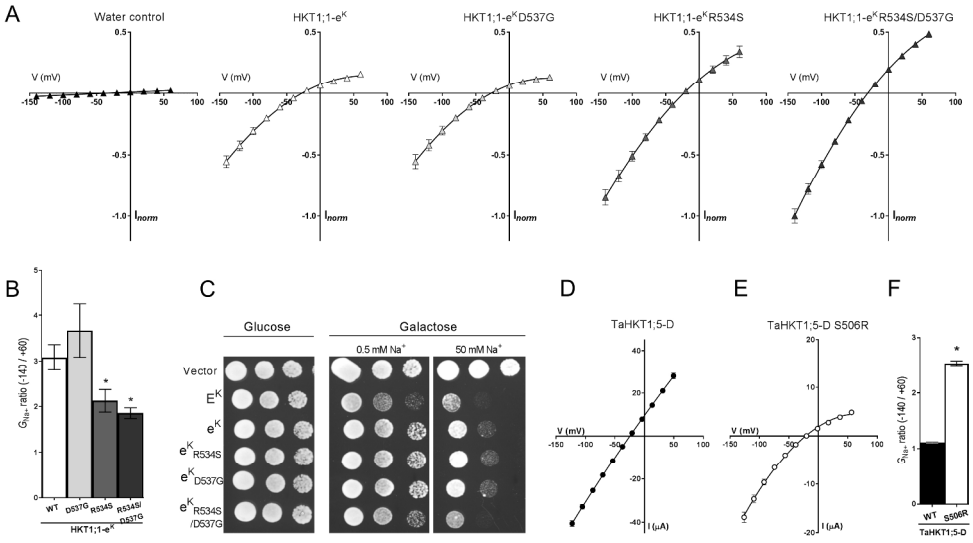

Figure 4: Arg-534 and Asp-537 control the gating and sodium conductance of VisHKT1;1-eK.

282x160mm (300 x 300 DPI)

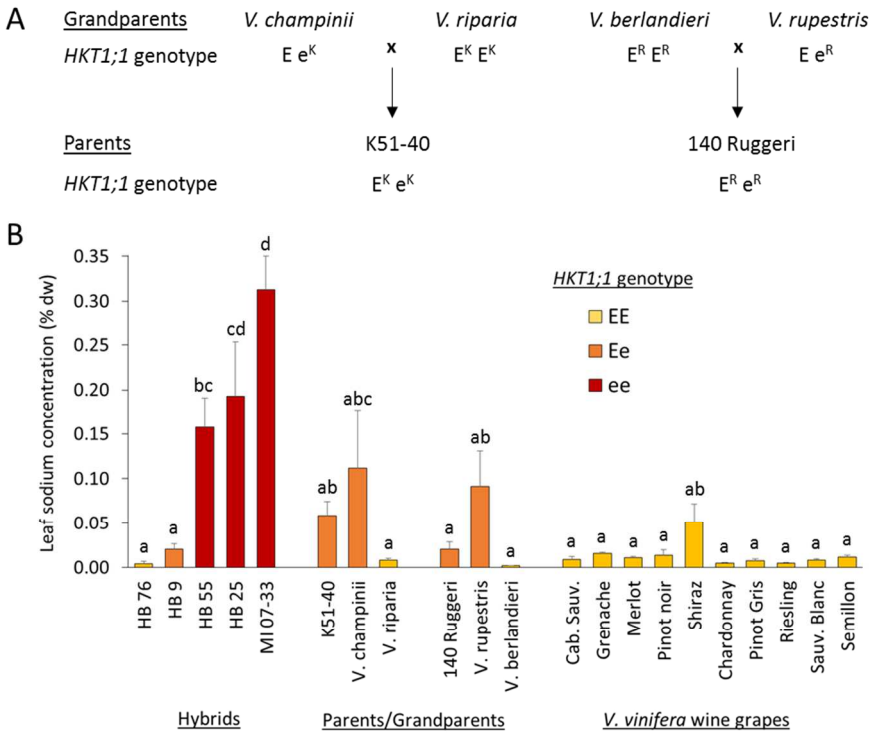

Figure 5: Recessive alleles, VisHKT1;1-eK and VisHKT1;1-eR, are derived from V. champinii and V. rupestris respectively.

254x190mm (300 x 300 DPI)